Journal of Sound and Vibration (2000) **238**(5), 877–892
doi:10.1006/jsvi.2000.3107, available online at http://www.idealibrary.com on IDEAL®

THE OPTIMIZATION TECHNIQUE-BASED BALANCING OF FLEXIBLE ROTORS WITHOUT TEST RUNS

B. Xu, L. Qu and R. Sun

Research Institute of Diagnostics and Cybernetics, Xi'an Jiaotong University Xi'an, Shaanxi, 710049, The People's Republic of China

(*Received* 12 *October* 1999, *and in final form* 31 *May* 2000)

In most balancing techniques currently in use, test weights and runs are required for the calculation of correction masses. This paper develops a new rotor balancing method without test runs, which uses the balancing objective of influence coefficient method and the initial phase point of Holospectrum. By calculating theoretical unbalance responses and measuring original unbalance vibrations, a new type of intelligent optimization technique, genetic algorithm, is applied to optimize the correction masses to minimize residual vibrations at selected measurement locations and balancing speeds. The implementation process and validity of this new method are discussed in detail through a numerical example, in which two cases are considered. In the field balancing experiment, a rotating rotor is balanced by employing the new method, in which average fluid oil coefficients within the balancing speeds are used in the calculation of unbalance responses, and the optimization correction masses are compared with those of the influence coefficient method. Both the simulation and experiment results show that this new method can reduce the residual vibrations effectively.

1. INTRODUCTION

Balancing of flexible rotors is one of the pivotal techniques in fault diagnosis of high-speed rotating machinery. It was shown that rotor unbalance was the main cause of increase of rotor vibrations. In most balancing procedures currently in use, test weights and runs are required for the calculation of correction masses, which consequentially increases balancing time and expenses. So the investigation of balancing method without test runs is a hot research field nowadays. Gnielka [1] and Morton [2] both proposed balancing procedures based on the modal balancing method, in which modal components of unbalances were identified without test runs to reduce the rotor vibrations. A new rotor balancing method based on the influence coefficient method and genetic algorithm is presented in this paper, in which reducing the residual vibrations is the direct optimization objective.

To introduce the theory, in section 2 the authors review briefly the well-established theory of the influence coefficient method, and discuss the relationships of the two methods. In section 3, the initial phase point of Holospectrum is introduced for describing the unbalance responses in this new method. The objective function is determined based on the balancing objective and optimization idea of the influence coefficient method in section 4. In section 5, the transfer matrix method and genetic algorithm are introduced for calculating unbalance responses and optimizing correction masses.

0022-460X/00/500877 + 16 $35.00/0

To show the implementation process and validity of this new method explicitly, in section 6, a simple numerical example is provided, in which two cases are considered. In case 1, rotor unbalances are identified satisfactorily, and in case 2, rotor residual vibrations are markedly reduced according to different balancing plane combinations.

In section 7, a rotating rotor is balanced by employing the new method, in which average fluid oil coefficients within balancing speeds are used for calculating unbalance responses, and the optimization correction masses are compared with those of the influence coefficient method. Both the simulation and experiment results show that this new method can reduce the residual vibrations effectively.

2. BALANCING STRATEGY

Rotor balancing is essentially a continuous optimization process of correction masses. Both the traditional modal balancing method [3] or the influence coefficient method [4] and their improvements [5–8] are to reduce rotor unbalances or vibrations by optimizing correction masses.

The influence coefficient method is a relatively mature and credible balancing technique widely used in mechanical industry, in which prior modal parameters are not necessary. In this method, correction masses are calculated by applying the least-squares method or the weighted least-squares method to solve the overdetermined linear equation system. The new balancing method presented in this paper uses the balancing objective and optimization idea of the influence coefficient method. Let us review briefly the theory of the influence coefficient method before we discuss this new balancing method.

When the rotor system is to be balanced by the influence coefficient method, the calculation equation of correction masses involved is

$$AU + S = 0, \tag{1}$$

where $A = [a^n_{mk}]_{L\times K}$ is the influence coefficient matrix, and $m = 1, 2, \ldots, M$: $k = 1, 2, \ldots, K$; $n = 1, 2, \ldots, N$; $L = M \times N$, $U = [u_1, u_2, \ldots, u_k]^{\mathrm{T}}$ the correction mass vector, $S = [s_1, s_2, \ldots, s_L]^{\mathrm{T}}$ the original vibration vector, a^n_{mk} the vibration of the mth measurement point caused by unit test weight in the kth balancing plane at the nth balancing speed and M, K, N the number of measurement points, number of balancing planes, number of balancing speeds.

The solutions of equation (1) are to find a set of correction masses U, so that the net responses AU of correction masses U can counteract the original vibrations S at the nth ($n = 1, 2, \ldots, N$) balancing speed entirely. When the condition $K < M \times N$ occurs, the equation system (1) is overdetermined, then the correction masses can be calculated by applying the least-squares method or the weighted least-squares method to minimize the residual vibrations. In this method, large numbers of test runs are required for forming the influence coefficient matrix A, which consequentially increases the balancing time and expenses.

The new balancing method presented uses the basic idea of influence coefficient method: reducing the residual vibrations is the direct balancing objective, and the correction masses are optimized by the basic idea of the least-squares or weighted least-squares method. We search a set of correction masses to make the responses of the correction masses counteracting original vibrations as much as possible in selected locations and speeds. The major difference between the two methods is that the new method requires no influence coefficient matrix, and optimizes the correction masses directly.

The main procedure of this new method is: by calculating the theoretic unbalance responses and measuring the original vibrations, the correction masses are optimized through the genetic algorithm to minimize the residual vibrations.

3. DESCRIPTION OF UNBALANCE RESPONSES

The measurement and description of unbalance responses are very important in rotor balancing procedures. In most traditional balancing methods, information on only one direction vibration in the measurement plane is used, which is based on the assumption that a rotor-bearing system has an equal rigidity in different directions, so big errors would occur when the rigidity is relatively different. Initial-phase point of Holospectrum [9, 10] effectively fuses information from two sensors in one measurement plane, and can describe the vibration states of rotor in the measurement plane entirely. For a rotor mounted in two bearings with a single disk, suppose that

$$x = x_0 \sin(\Omega t + \alpha), \qquad y = y_0 \sin(\Omega t + \beta) \tag{2}$$

is the synchronous response component of signals picked up from two orthogonal directions X and Y, and is uniformed with key-phase signal, where x_0, y_0 are amplitudes, α, β are initial phases, Ω is rotational speed and t is time. Equation (2) can be regarded as the equation of rotor synchronous rotating orbit. The initial-phase point of Holospectrum is defined as

$$I_0 = \sqrt{(x \sin\alpha)^2 + (y_0 \sin\beta)^2} \angle \operatorname{arctg} \frac{y_0 \sin\beta}{x_0 \sin\alpha}. \tag{3}$$

From equation (3), we can see that the initial-phase point fully considers information from two directions, and can accurately describe the characteristic of rotor vibrations. In this paper I_0 will be used as the description of unbalance responses in the new balancing process.

4. OPTIMIZATION OBJECTIVE

Supposing the rotor original vibrations are *Svector*, and theoretic net responses only caused by correction masses are $Tvector(u_k)$ (u_k is the correction mass in the kth balancing plane, $k = 1, 2, \ldots, K$), complex residual vibration vector is defined as

$$\varepsilon(u_k) = Svector + Tvector(u_k) = \begin{bmatrix} svector_1^1 + tvector_1^1(u_k) \\ svector_2^1 + tvector_2^1(u_k) \\ \vdots \\ svector_M^1 + tvector_M^1(u_k) \\ \vdots \\ svector_m^n + tvector_m^n(u_k) \\ \vdots \\ svector_M^N + tvector_M^N(u_k) \end{bmatrix} = \begin{bmatrix} \varepsilon_1(u_k) \\ \varepsilon_2(u_k) \\ \vdots \\ \varepsilon_M(u_k) \\ \vdots \\ \varepsilon_l(u_k) \\ \vdots \\ \varepsilon_L(u_k) \end{bmatrix}, \tag{4}$$

where the definitions of M, N, K are the same as those in equation (1), and $L = M \times N$. The optimization objective function can be defined as follows by using the optimization idea of the least-squares or weighted least-squares method.

(1) Minimize the sum of squares of residual vibration components:

$$J = \min \sum_{l=1}^{L} |\varepsilon_1(u_k)|^2. \tag{5}$$

(2) Minimize the modulus of maximal residual vibration component:

$$J = \min \|\varepsilon\|_\infty = \min\left(\max_{1 \leqslant l \leqslant L} |\varepsilon_1(u_k)| \right). \tag{6}$$

The restrictions of equations (5) and (6) are

$$\text{s.t. } \text{mod}(u_k) \subseteq (0, H_k), \qquad \arg(u_k) \subseteq (0, 2\pi) \quad k = 1, 2, \ldots, K, \tag{7}$$

where mod represents the modulus of a complex number, and arg represents the phase angle of a complex number. H_k represents the upper limit of correction mass permitted in the kth balancing plane.

5. IMPLEMENTATION OF OPTIMIZATION

5.1. CALCULATION OF UNBALANCE RESPONSES

The calculation methods of rotor unbalance responses are relatively numerous and mature. Generally speaking, all methods widely used in engineering can be classified into two categories: the transfer matrix method [11] and the finite element method (FEM). The advantage of the transfer matrix method is that the dimension of transfer matrix does not increase when the degrees of freedom of a rotor system rise, and it is convenient to programme. So in this paper, the transfer matrix method is used in the calculation of unbalance responses.

In the transfer matrix method, a rotor system is first divided into several typical parts, such as disks, shafts, bearings, etc. Supposing $\{z\}_i$ is the state vector of the ith rotor cross-section, then each state vector has a certain relationship:

$$\{Z\}_{i+1} = [T]_i \{z\}_i = [T]_i [T]_{i-1} \cdots [T]_1 \{z\}_1, \tag{8}$$

where $[T]_i$ is the transfer matrix of the ith typical part. When $\{z\}_i$ has r elements, the dimension of $[T]_i$ is $r \times r$.

By calculating vibrations caused by unbalances at a certain rotational speed, we can get the unbalance reponses. If the anisotropic stiffness is considered, the state vector can be as follows:

$$\{z\}_i = \{x, \theta_y, M_y, Q_x, y, -\theta_x - M_x, Q_y, 1\}_i^{\mathrm{T}}, \tag{9}$$

where x, y are displacement, θ_x, θ_y are slopes, M_x, M_y are bending moments, and Q_x, Q_y are shearing forces.

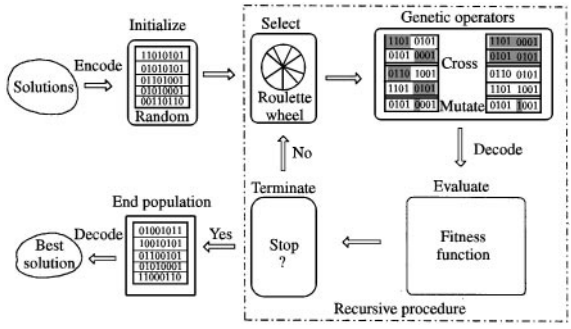

Figure 1. The framework of GA.

5.2. INTELLIGENT OPTIMIZATION TECHNIQUES

Optimization of correction masses is a complex non-linear problem, and there are many optimization techniques that can solve this kind of problem. Some new intelligent optimization techniques, such as genetic algorithm [12], neural network and simulated annealing, have been successfully applied to optimize the problem in many fields. In this paper, the genetic algorithm (GA) will be used to optimize the correction masses because of its superiority in this field.

(1) GA uses a population-based search strategy, so it can find global optimum solution with high probability.

(2) GA does not depend on the gradient information of the objective function, and only requires the fitness information, which can provide the quantity to evaluate the colonies. GA is especially suitable for a complex non-linear problem. For example, the objective functions are of high order, cannot be differentiated and so on.

(3) GA is robust for various real-world problems.

The optimization of GA is essentially a recursive process, and the basic framework of GA is shown in Figure 1. Combining our optimization problem, the implementation of GA is as follows:

(1) *Encode*: Encoding the solutions is the first step in GA, which establishes the relationship between solutions and chromosomes. Generally speaking, there are two kinds of encodes: float and binary. Float encode is used in this paper because of its advantages, such as high speed and accurate calculation, abundant genetic operators, and so on.

(2) *Initialize*: One of the most important characteristics of GA is to operate with the colonies. So it needs to initialize the solutions with colonies before the evolution.

(3) *Selection*: Selection operation in GA resembles the mechanism in biology. Colonies with good "properties" have more chances of survival than bad ones.

(4) *Genetic operation*: The core part in GA is the genetic operation. By crossing and mutating among individuals, the colonies can keep the information variable.

(5) *Evaluate*: Fitness function provides the tool for colony evaluation. Here we can use the objective function of rotor balancing as the fitness function.

(6) *Terminate*: Here the maximum evaluation generation provides the termination.

6. NUMERICAL EXAMPLE

In this section, we will treat a numerical example in order to discuss the implementation process and validity of the proposed method explicitly. Before the discussion, we first define

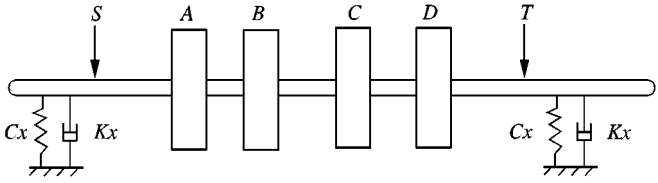

Figure 2. Configuration of the numerical example.

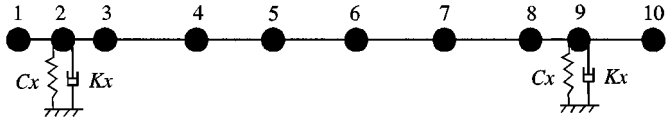

Figure 3. Theoretical model of the numerical example.

TABLE 1

The configuration parameters of the numerical example

	Configuration parameters
Disk	Diameter: 80 mm Thickness: 30 mm Mass: 900 g
Set radius of weight mass	$r = 36$ mm
Bearing	K_x: $1{\cdot}40106 \times 10^5$ N/m K_y: $1{\cdot}75133 \times 10^5$ N/m
	C_x: 12·26 kg/s C_y: 17·51 kg/s
Shaft	Diameter: 15 mm Density: 7800 kg/m^3
	Modulus of Elasticity: $2{\cdot}1 \times 10^{11}$ N/m^2
Co-ordinates of nodes	$L1 = 0$ mm $L2 = 45$ mm $L3 = 80$ mm $L4 = 170$ mm $L5 = 240$ mm $L6 = 330$ mm $L7 = 410$ mm $L8 = 500$ mm $L9 = 540$ mm $L10 = 620$ mm

two conceptions for the sake of convenience in description: If equations (5) and (7) are employed as the optimization function, we may call it "Method 1". Similarly, we may entitle the process "Method II", in which equations (6) and (7) are selected as the optimization function.

6.1. SIMULATION MODEL

A simple flexible rotor with continuous mass distribution, which is shown in Figure 2, is chosen as the numerical example model. In Figure 2, *A*, *B*, *C* and *D* are four identical disks, and *S*, *T* are two measuring plane locations of the rotor vibrations. For simplifying the analysis, we suppose that the set radius of initial unbalance masses and correction masses in disks is fixed i.e., $r = 36$ mm. The theoretical model of this rotor is also established, which is shown in Figure 3. The configuration parameters are listed in Table 1 for the theoretical calculations of the rotor critical speeds and unbalance responses. The four calculated critical speeds are 1871, 5374, 10 589 and 16 905 r/min.

In this section, two different cases are considered, in which both Methods I and II will be applied. In case one, we suppose that the locations of the disks, on which the initial unbalances exist, are known, so the balancing planes are selected as these disks. In this case,

TABLE 2

GA parameters

	Parameters
Fitness function	$\max\left(-\sum_{l=1}^{L}\lvert\varepsilon_l(u_k)\rvert^2\right)$ $k=1,2$ $L=M\times N=2\times 6=12$
Search space of the variable	$\mathrm{mod}(u_k)\subseteq(0,3)$ g $\arg(u_k)\subseteq(0,2\pi)$ rad $k=1,2$
Number of colonies	80
Maximum evolution generation	20

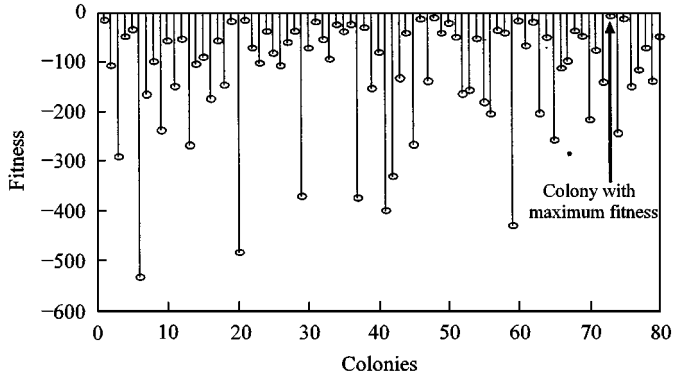

Figure 4. The fitness of the initial colonies.

rotor unbalances can be identified satisfactorily by employing the new method. In case two, we assume that the unbalance locations are not known, so the balancing planes may not be coincident with these unbalance disks entirely, and in this case, the residual vibrations are markedly reduced according to different selected balancing planes.

6.2. CASE 1

In this case, we suppose that the rotor initial unbalance masses, which are listed in Table 3, are only on disks A and C, and the two balancing planes are also selected as disks A and C.

Method 1 will be discussed in detail here to illustrate the optimization processes explicitly. Firstly, six balancing speeds are selected which are listed in Table 4 and the upper limit of correction mass permitted in the kth ($k = 1, 2$) balancing plane H_k is assumed as 3 g.

In the genetic algorithm, the fitness function is the only evaluation tool for different colonies, in which the bigger the fitness, the better the colony is. Because the calculation of equation (5) is the minimizing process of the objective function and the result is always positive, we can transform equation (5) into the fitness function form listed in Table 2. A similar transformation will be necessary if equation (6) is employed. All the parameters necessary in GA are listed in Table 2.

According to the parameters shown in Table 2, 80 initial colonies are produced randomly and their fitness values are shown in Figure 4. In Figure 4, we can see that the initial colonies are not desirable because their fitness values are very small with average fitness $-123{\cdot}32$ and maximum fitness $-6{\cdot}76$. In Figure 4, the colony with the maximum fitness is

TABLE 3

Rotor unbalance masses and correction masses (g@°)

	Original unbalance masses	Correction masses	
		Method I	Method II
Disk *A*	$U_A = 0{\cdot}80@100{\cdot}00$	$P_A = 0{\cdot}80@279{\cdot}68$	$P_A = 0{\cdot}80@279{\cdot}96$
Disk *C*	$U_C = 1{\cdot}20@230{\cdot}00$	$P_C = 0{\cdot}19@50{\cdot}29$	$P_C = 1{\cdot}20@50{\cdot}03$
Fitness	—	$-8{\cdot}3 \times 10^{-4}$	$-2{\cdot}5 \times 10^{-3}$

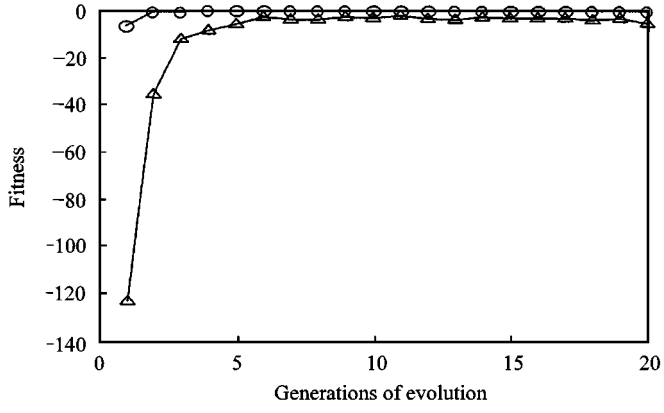

Figure 5. Curve of fitness corresponding to evolution generations: ○—○ maximum fitness; △—△ average fitness.

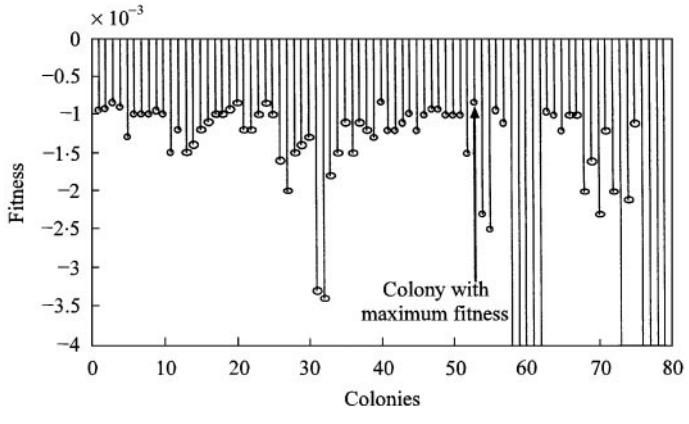

Figure 6. The fitness of the colonies after 20 evolution generations.

marked. In the later GA processes, the colonies are evolving through genetic operations, i.e., crossing, mutating and selection, and Figure 5 shows the curve of fitness corresponding to the whole evolving process. In Figure 5, we can see that the maximum fitness of each evolution generation is increasing when the evolution continues, but the evolution ability decreases after the first five evolution generations. After 20 evolution generations, the colonies are fairly good with much higher fitness as shown in Figure 6. In Figure 6, the

TABLE 4

Initial-phase points of the two types of vibrations in Method I (μm@$^\circ$)

Balancing speeds (r/min)	Initial-phase points in disk S		Initial-phase points in disk T	
	Original vibrations	Theoretical responses of correction masses	Original vibrations	Theoretical responses of correction masses
$\Omega_1 = 1300$	1·68@179·91	1·65@−0·36	1·87@−162·18	1·84@17·87
$\Omega_2 = 2100$	8·46@33·18	8·31@−146·85	7·56@25·02	7·41@−155·18
$\Omega_3 = 2500$	4·13@35·49	4·07@−144·35	2·88@−2·57	2·82@176·94
$\Omega_4 = 3000$	4·22@45·82	4·18@−133·91	2·30@−28·95	2·27@150·19
$\Omega_5 = 4600$	33·64@17·02	33·56@−162·98	30·66@−165·51	30·07@14·49
$\Omega_6 = 5600$	38·77@−82·44	38·74@97·49	46·28@90·14	46·15@−89·81

average fitness is $-5{\cdot}67$ and the maximum fitness is $-8{\cdot}3\times10^{-4}$. The best colony with the maximum fitness is marked in Figure 6, which is also the final optimization result of the correction masses listed in Table 3, i.e., $P_A = 0{\cdot}80$g@279·68 and $P_C = 1{\cdot}19$g@50·29. Table 4 shows the initial-phase points of original vibrations and vibrations only caused by the optimization correction masses in six balancing speeds in Method I, we can see that the two types of vibrations are satisfactorily counteractive.

We can also use Method II to calculate the correction masses. The rotor initial unbalance masses and correction masses are all listed in Table 3. We can see that the results of both methods are excellent.

6.3. CASE 2

In this case, we suppose that the four disks all have unbalance masses with different amplitudes and phases as follows:

$$U_A = 0{\cdot}80@100{\cdot}00, \qquad U_B = 0{\cdot}20@230{\cdot}00, \qquad U_C = 0{\cdot}40@0{\cdot}00,$$

$$U_D = 0{\cdot}50@310{\cdot}00 \qquad (g@^\circ).$$

For simplifying the discussion, we restrict out analysis to three balancing planes for rotor balancing, so there are four different combinations of balancing planes, i.e., *ABC*, *ACD*, *BCD*, *ABD*. The balancing speeds are the same as those in case 1. The number of colonies is 90 and the maximum evolution generation is 30. The optimization correction masses and their fitness, which are calculated from different balancing plane combinations, are listed in Table 5.

Figure 7 shows the original vibration amplitude and residual vibration amplitude calculated from eight different correction masses listed in Table 5, and we can see that all the residual vibrations are decreased effectively. In order to compare the results of different balancing plane combinations calculated by Method II, we plot the curve of the residual vibration amplitude, which is shown in Figure 8. We can see that the balancing results of plane *ABC* combination are relatively good.

TABLE 5

Correction masses and fitness calculated from different balancing plane combinations (g@°)

Balancing planes	Method	Correction masses			Fitness
ABC	Method I	$P_A = 0{\cdot}54@278{\cdot}65$	$P_B = 1{\cdot}17@9{\cdot}84$	$P_C = 1{\cdot}24@139{\cdot}64$	−0·0191
	Method II	$P_A = 0{\cdot}57@292{\cdot}97$	$P_B = 0{\cdot}97@10{\cdot}92$	$P_C = 1{\cdot}15@135{\cdot}52$	−0·0809
ACD	Method I	$P_A = 0{\cdot}35@284{\cdot}09$	$P_C = 1{\cdot}18@40{\cdot}25$	$P_D = 1{\cdot}18@174{\cdot}22$	−0·1769
	Method II	$P_A = 0{\cdot}46@340{\cdot}45$	$P_C = 0{\cdot}79@15{\cdot}65$	$P_D = 0{\cdot}94@148{\cdot}59$	−0·2256
BCD	Method I	$P_B = 0{\cdot}27@335{\cdot}87$	$P_C = 0{\cdot}76@21{\cdot}52$	$P_D = 1{\cdot}21@152{\cdot}48$	−0·2482
	Method II	$P_B = 0{\cdot}56@348{\cdot}11$	$P_C = 0{\cdot}45@55{\cdot}73$	$P_D = 0{\cdot}93@145{\cdot}73$	−0·1915
ACD	Method I	$P_A = 0{\cdot}15@251{\cdot}77$	$P_B = 0{\cdot}61@13{\cdot}76$	$P_D = 0{\cdot}95@138{\cdot}27$	−0·2428
	Method II	$P_A = 0{\cdot}06@241{\cdot}23$	$P_B = 0{\cdot}61@\ 7{\cdot}67$	$P_D = 0{\cdot}97@134{\cdot}71$	−0·2017

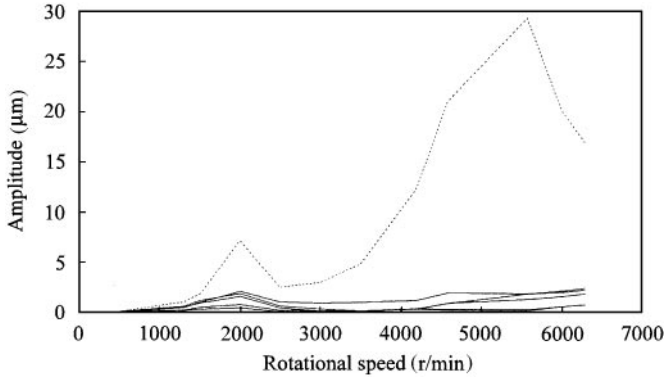

Figure 7. Rotor original vibrations and residual vibrations calculated from eight different correction masses listed in Table 5: ..... original vibrations; —— residual vibrations.

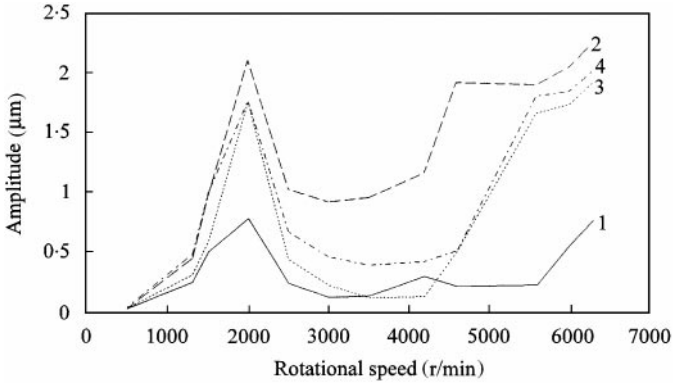

Figure 8. Residual vibrations of different balancing plane combinations calculated by Method II: —— 1 plane *ABC*; – – – – 2 plane *ACD*; ..... 3 plane *BCD*; – · – · – · – 4 plane *ABD*.

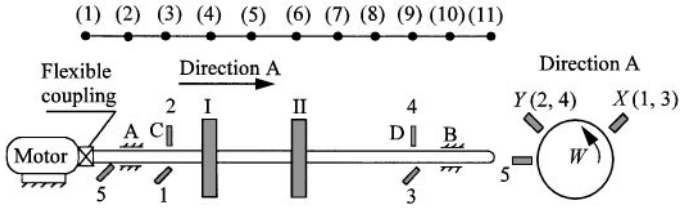

Figure 9. Configuration of the test rig.

TABLE 6

The configuration parameters of rotor-bearing system

	Configuration parameters
Balancing planes I, II	Diameter: 60 mm Thickness: 25 mm Mass: 800 g
Bearing A, B	Average stiffness: $5{\cdot}75133 \times 10^5$ N/m Average damping: 17·51 kg/s
Shaft	Diameter: 10 mm Density: 7800 kg/m^3 Modulus of Elasticity: $2{\cdot}1E \times 10^{11}$ N/m^2
Co-rdinates of nodes	$L1 = 0$ mm $L2 = 32$ mm $L3 = 67$ mm $L4 = 134$ mm $L5 = 203$ mm $L6 = 272$ mm $L7 = 333$ mm $L8 = 382$ m m $L9 = 443$ mm $L10 = 477$ mm $L11 = 549$ mm

7. BALANCING EXPERIMENT

In this section, the proposed method will be applied in field balancing experiment. The configuration of test rig is show in Figure 9, where 1–5 are the displacement probes, and 1–4 measure the vibrations in two measurement planes C and D near two bearings A and B, and 5 is the key phase probe. I and II are two balancing planes. To model the rotor system, the rotor-bearing system is divided into 11 nodes as shown in Figure 9. By the calculation, the first critical speed is 1964 r/min (2000 r/min measured in the experiment), and the second critical speed is 7888 r/min. The configuration parameters are listed in Table 6.

The original vibrations are measured at different speeds when the rotor runs up, which are shown in Figure 14 represented by "○". Five balancing speeds, which should escape from the rotor-bearing unstable speed range, are selected: 1100, 2300, 3100, 3700, and 4300 r/min. We select two balancing planes I and II, and two measurement planes C and D. The optimization objective is composed of equations (5) and (7), i.e., Method I. Because the maximum mass permitted in the balancing plane is 3 g, the parameter $H_k = 3$ g ($k = 1, 2$). In the balancing experiment, the average stiffness and damping within the balancing speeds are used in the optimization process of correction masses.

The genetic algorithm is applied to optimize the correction masses. The number of initial colonies is selected as 80, and the maximum evolution generation is 20. The curve of fitness corresponding to the evolution generations is shown in Figure 10. We can see that it is very effective in the first five generations, and the evolution ability decreases in the latter generations. The fitness is -8087 at the 20th generation. The initial phase points of theoretical net responses (represented by "□") only caused by correction masses and those of the measured original vibrations (represented by "○") in five balancing speeds are shown in Figure 11. It can be seen that, the two kinds of vibrations are counteractive

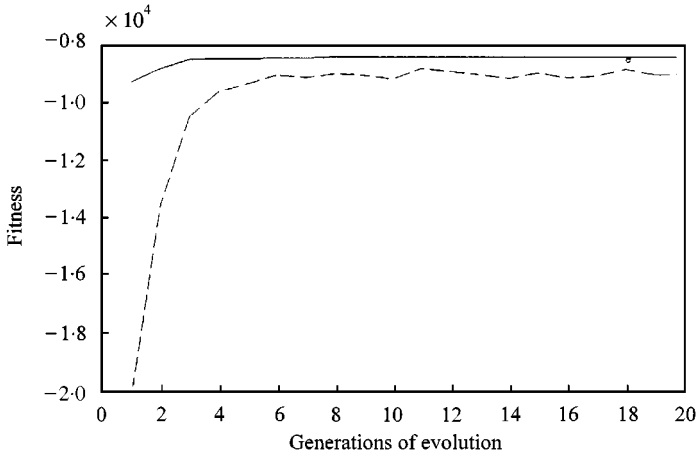

Figure 10. Curve of fitness corresponding to evolution generation: —— maximum fitness; – – – – average fitness.

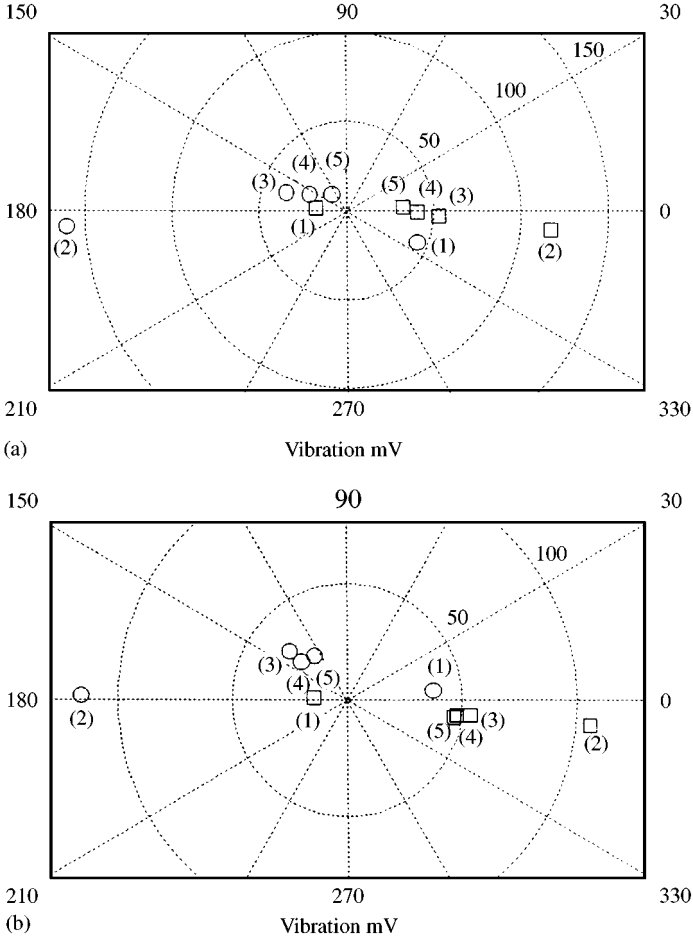

Figure 11. The initial phase points of the theoretical net responses of correction masses and those of the measure original vibrations in five balancing speeds. (a) The initial-phase points in measurement plane C. (b) The initial-phase points in measurement plane D: ○—○ *Svector*; □—□ *Tvector*; (1)–(5) Five balancing speeds.

TABLE 7

The correction masses calculated in the experiment

		Balancing without test runs	Influence coefficient method
Two balancing planes	Scheme 1: planes I and II	$P_1 = 0{\cdot}64\text{g}@-300{\cdot}20$ $P_2 = 0{\cdot}52\text{g}@-290{\cdot}93$	$P_1 = 0{\cdot}68\text{g}@-305{\cdot}72$ $P_2 = 0{\cdot}46\text{g}@-291{\cdot}31$
Single balancing plane	Scheme 2: plane I	$P_1 = 1{\cdot}27\text{g}@-295{\cdot}61$	$P_1 = 1{\cdot}24\text{g}@-302{\cdot}01$
	Scheme 3: plane II	$P_2 = 0{\cdot}86\text{g}@-294.61$	$P_2 = 0{\cdot}86\text{g}@-294{\cdot}57$

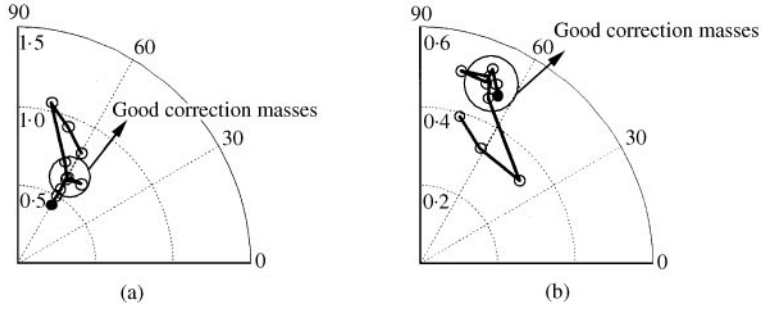

Figure 12. Distributions of correction masses with different stiffness: (a) correction masses in plane I; (b) correction masses in plane II.

approximately. The optimization correction masses are reasonable, which are listed in Table 7, and the balancing results are shown in Figure 14 represented by "□".

The mathematical model of the rotor system is necessary in the calculation of the unbalance responses, in which the reasonable considerations of the dynamic coefficients of fluid oil are very important. The average stiffness and damping are used to calculate the unbalance responses in the proposed method, and it can be seen from Figure 14 that the balancing results are fairly satisfactory. Many beneficial works have been done for obtaining the fluid oil coefficients [13, 14]; however, in some cases we could not obtain the precise average values easily. In order to study the influence of variations of the two dynamic coefficients in the vicinity of the average values on the correction masses, respectively, simple analysis experiments are conducted as follows.

(1) Keep the average damping unvaried, and permit stiffness to vary in the vicinity of the average value.

The relatively broad variable scope of stiffness is $K \subseteq [2{\cdot}05133E + 5\ 8{\cdot}75133E + 5]$ N/m, 10 stiffnesses in this scope are equal space selected for the calculation of correction masses. The distributions of calculated correction masses are shown in Figure 12. The polar co-ordinate in Figure 12 represents the balancing plane, in which co-ordinate angle represents the angle of correction masses in the balancing planes, and the co-ordinate magnitude represents the mass of correction weight (the set radius of correction masses in balancing plane is fixed, i.e., $r = 26$ mm). "○" represents the correction of mass calculated by different stiffnesses, and "●" represents that of the least stiffness. The lines represent the increasing of the stiffness. It can be seen that the influence of the variations of the stiffness in the vicinity of the average value on the correction masses is not so remarkable, and several good correction masses are marked.

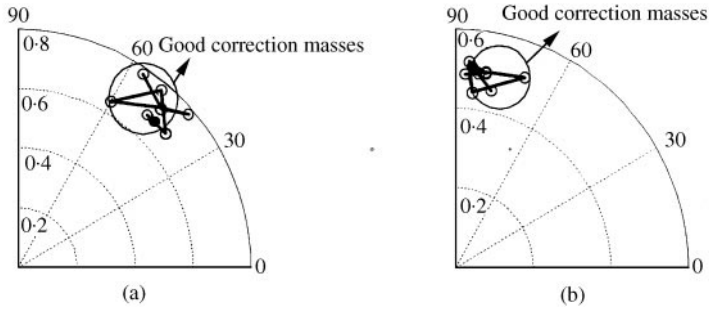

Figure 13. Distributions of correction masses with different dampings: (a) correction masses in plane I; (b) correction masses in plane II.

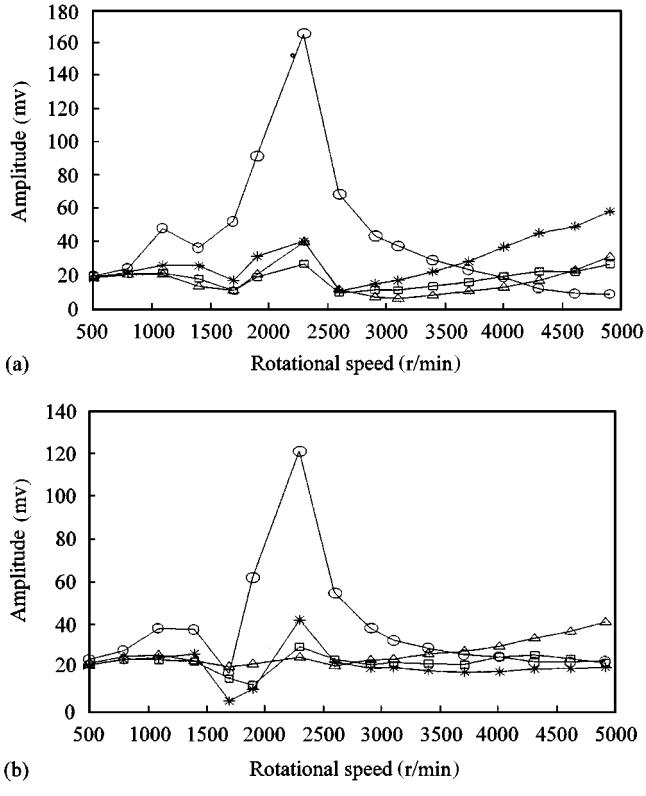

Figure 14. Vibrations in different rotor runs. (a) The vibrations in measurement plane C. (b) The vibrations in measurement plane D: ○—○ original vibrations; □—□ residual vibrations in scheme 1; △—△ residual vibrations in scheme 2; ∗—∗ residual vibrations in scheme 3.

(2) Keep the average stiffness unvaried, and permit damping to vary in the vicinity of the average value.

The relatively broad variable scope of damping is $C \subseteq [3{\cdot}502\ 31{\cdot}521]$ kg/s, 10 dampings in this scope are equal space selected for the calculation of correction masses. The distributions of correction masses are shown in Figure 13. The meaning of identifiers in Figure 13 are the same as those in Figure 12 (damping instead of stiffness here). It can be

seen that the influence of the variations of the damping in the vicinity of the average value on the correction masses is relatively small, and several good correction masses are marked.

We balance the rotor system by using both single- and double-balancing planes, in which the optimization objectives are all composed of equations (5) and (7). The optimization results are listed in Table 7. We also use the influence coefficient method to balance the rotor-bearing system, and the correction masses calculated are also listed in Table 7. It can be seen that the correction masses calculated from the two balancing methods are very close. The vibration amplitudes, before and after correction by different balancing scheme, are shown in Figure 14, in which "○" represents the original vibration, "□" represents the residual vibration in scheme 1, "△" and "*" represent the residual vibrations in scheme 2 and scheme 3, respectively. It can be seen that the original vibrations are reduced effectively within the scope of the considered balancing speeds. But with the rising of the rotating speed close to the second critical speed, the residual vibrations of schemes 2 and 3 increase, because the second modal component of unbalances cannot be balanced well by a single balancing plane. The balancing result of scheme 1 is better than that of schemes 2 and 3.

8. CONCLUDING REMARKS

This present paper is devoted to the development of a new rotor balancing method without test weights. The key feature of the proposed method is that the genetic algorithm and the Holospectrum technique are employed in the optimization process of the traditional influence coefficient method. By calculating theoretical unbalance responses and measuring original unbalance vibrations, the genetic algorithm is applied to optimize the correction masses to minimize residual vibrations at selected measurement locations and balancing speeds. Both the simulation and experiment results show that this new method can reduce the residual vibrations effectively.

REFERENCES

1. P. GNIDLKA 1983 *Journal of Sound and Vibration* **90**, 157–172. Modal balancing of flexible rotors without test runs: an experimental investigation.
2. P. G. MORTON 1985 *Proceedings of the Institution of Mechanical Engineers* **199**, 71–78. Modal balancing of flexible shafts without trial weights.
3. W. KELLENBERGER 1972 *Journal of Engineering for Industry. Transaction of the American Society of Mechanical Engineers* **94**, 548–560. Should a flexible rotor be balanced in N or $(N + 2)$ planes?
4. T. P. GOODMAN 1964 *Journal of Engineering for Industry, Transaction of the American Society of Mechanical Engineers* **86**, 273–279. A least-squares method for computing balance corrections.
5. G. PARKINSON, M. S. DARLOW and A. J. SMALLEY 1980 *Journal of Sound and Vibration* **68**, 489–506. A theoretical introduction to the development of a unified approach to flexible rotor balancing.
6. S. SAITO and T. AZUMA 1983 *Journal of Vibration, Acoustics, Stress, and Reliability in Design, Transaction of the American Society of Mechanical Engineers* **105**, 94–100. Balancing of flexible rotors by the complex modal method.
7. S.-G. TAN and X.-X. WANG 1993 *Journal of Sound and Vibrations* **168**, 385–394. A theoretical introduction to low speed balancing of flexible rotors: unification and development of the modal balancing and influence coefficient techniques.
8. V. STEFFEN JR. and H. B. LACERDA 1996 *Modal Analysis* **11**, 96–105. The balancing of flexible rotors.
9. L. S. QU, Y. D. CHENG and X. LIU 1989 *Mechanical System and Signal Processing* **3**, 255–267. The holospectrum: a new method for surveillance and diagnosis.

10. L. S. QU, H. QIU and G. H. XU 1998 *China Mechanical Engineering* **9**, 60–63 Rotor balancing based on holospectrum analysis: principle and practice (in Chinese).
11. G. C. HORNER, W. D. PILKEY 1978 *Journal of Mechanical Designs, Transaction of the American Society of Mechanical Engineers* **100**, 297–302. The riccati transfer matrix method.
12. D. E. GOLDBERG 1989 *Genetic Algorithms in Search, Optimization and Machine Learning*. Reading, MA: Addison-Wesley.
13. Y. Y. ZHANG, Y. B. XIE, D. M. QIU 1992 *Journal of Sound and Vibration* **152**, 531–547. Identification of linearized oil-film coefficients in a flexible rotor-bearing system. Part I. Model and simulation.
14. Y. Y. ZHANG, Y. B. XIE, D. M. QIU 1992 *Journal of Sound and Vibration* **152**, 549–559. Identification of linearized oil-film coefficients in a flexible rotor-bearing system. Part II. Experiment.